

# **Temperature Adjustment of Surface Curvature Index Computed from Traffic Speed Deflectometer Measurements (SCI<sub>TSD</sub>)**

## **Mahdi Nasimifar, Corresponding Author**

NRC Research Associate

Federal Highway Administration

Turner Fairbank Highway Research Center

6300 Georgetown Pike, McLean, VA 22101

Tel: (202) 493-3404 ; Fax: (202)493-3161; Email: [s.nasimifar.ctr@dot.gov](mailto:s.nasimifar.ctr@dot.gov)

## **Sarah Chaudhari**

Intern at FHWA through TWC

Federal Highway Administration

Turner-Fairbank Highway Research Center

6300 Georgetown Pike, McLean, VA 22101

Tel: (412) 860-0120; Email: [skc31@pitt.edu](mailto:skc31@pitt.edu)

## **Senthilmurugan Thyagarajan**

Research Civil Engineer, ESC Inc.

Turner Fairbank Highway Research Center

6300 Georgetown Pike, McLean, VA 22101

Tel: (202) 493-3157 ; Fax: (202) 493-3161; Email: [senthil.thyagarajan.ctr@dot.gov](mailto:senthil.thyagarajan.ctr@dot.gov)

## **Nadarajah Sivaneswaran**

Senior Civil Research Engineer

Federal Highway Administration

Turner Fairbank Highway Research Center

6300 Georgetown Pike, McLean, Virginia, VA 22101

Tel: (202) 493-3147; Fax: (202) 493-3161; Email: [nadarajah.sivaneswaran@dot.gov](mailto:nadarajah.sivaneswaran@dot.gov)

**Abstract**

Pavement structural condition evaluation plays an important role in assessing rehabilitation needs and making prudent investment decisions. Deflection testing serves as the most commonly used pavement structural condition evaluation technique. Of late, use of traffic speed deflection devices, such as Traffic Speed Deflectometer (TSD), are being considered especially at the network level for pavement management applications. For asphalt concrete (AC) pavements, Surface Curvature Index computed from TSD measurements ( $SCI_{TSD}$ ), is a widely-used index for assessing the structural condition of the AC layers. Since asphalt modulus is temperature sensitive, measured deflections and consequently the computed  $SCI_{TSD}$  are also affected by pavement temperature at the time of testing. For consistent pavement evaluation,  $SCI_{TSD}$  computed across sections and over time should be adjusted to a reference temperature.

This study presents an applied method for adjusting  $SCI_{TSD}$  to a reference temperature. The method was based on a model developed from a dataset built from responses computed with dynamic-viscoelastic analyses under TSD moving load in a wide range of pavement properties. The method was field evaluated with TSD data from three locations within the US and one location each in Europe and Australia. The US locations include the Minnesota Department of Transportation's MnROAD pavement test track facility and one in-service pavement sections each in Virginia and Illinois. The results showed that the proposed method can reasonably adjust  $SCI_{TSD}$  to a reference temperature which enables its application in pavement structural assessment and subsequent use in pavement management activities.

**Keywords:** Surface curvature index, Temperature adjustment, Viscoelastic analyses, Traffic speed deflectometer, Pavement management system

## Introduction

Pavement structural evaluation is an important component of in-service pavement assessment that highway agencies undertake in determining pavement rehabilitation needs. Vertical surface deflections from Falling Wheel Deflectometer (FWD) is the most common structural response that provide the inputs for structural analysis of in-service pavements and for the planning of maintenance and rehabilitation (M&R) strategies.

Deflection basin indices derived from vertical surface deflections are known to be simple yet good indicators of pavement structural condition. Their merit in pavement analysis and pavement management system applications have been documented in several studies [1-3]. Surface Curvature Index (SCI) is one such deflection basin indices that has been shown to be a good predictor of horizontal tensile strain at the bottom of the asphalt layer ( $\epsilon_t$ ), a critical response used to predict asphalt concrete (AC) pavement fatigue performance [3].

Recently, traffic speed deflection devices (TSDDs), such as Traffic Speed Deflectometer (TSD) and Rolling Wheel Deflectometer (RWD), have made pavement structural evaluation practical at the network level for pavement management applications [4]. TSDDs, such as TSD, are globally gaining importance, as they can measure near continuous surface deflections at traffic speed to overcome the limitations of FWD, such as stop-and-go operation, lane closures, and slow rate of testing, especially for network level pavement management applications. TSD is equipped with Doppler lasers along the midline of rear dual tires (Figure 1a) that measure pavement deflection velocities. The TSD device used in this study was equipped with seven Doppler lasers - one for reference and others to measure deflection velocities at six locations: 100, 200, 300, 600, 900 and 1500 mm in front of the rear dual tires (Figure 1a). The surface deflections are then computed from measured deflection velocities (Figure 1b) through one of several available methods (Figure 1c) [5,6]. SCI computed from TSD measurements referred to hereafter as  $SCI_{TSD}$  is defined as the difference between deflections at the midpoint between dual tires ( $D_0$ ) and at 300 mm from that point ( $D_{300}$ ) as shown in Figure 1c.

$SCI_{TSD}$  was identified as one of the most robust indices to estimate maximum horizontal strain at the bottom of the AC layer [4]. Katicha et al [7] categorized pavement structural condition at network level into Good, Fair, and Poor using  $SCI_{TSD}$ . The  $SCI_{TSD}$  is also a widely-used index in Europe for assessing bearing capacity characteristics of pavements at network level with TSD data [8, 9]. Baltzer compared  $SCI_{TSD}$  in different years and showed that it increased year by year in a pavement section indicating a decrease in bearing capacity [10]. For the use of  $SCI_{TSD}$  in pavement management activities, the index measured at different temperatures should be adjusted to a reference temperature. The objective of this study is to introduce a field validated temperature adjustment method for this purpose.

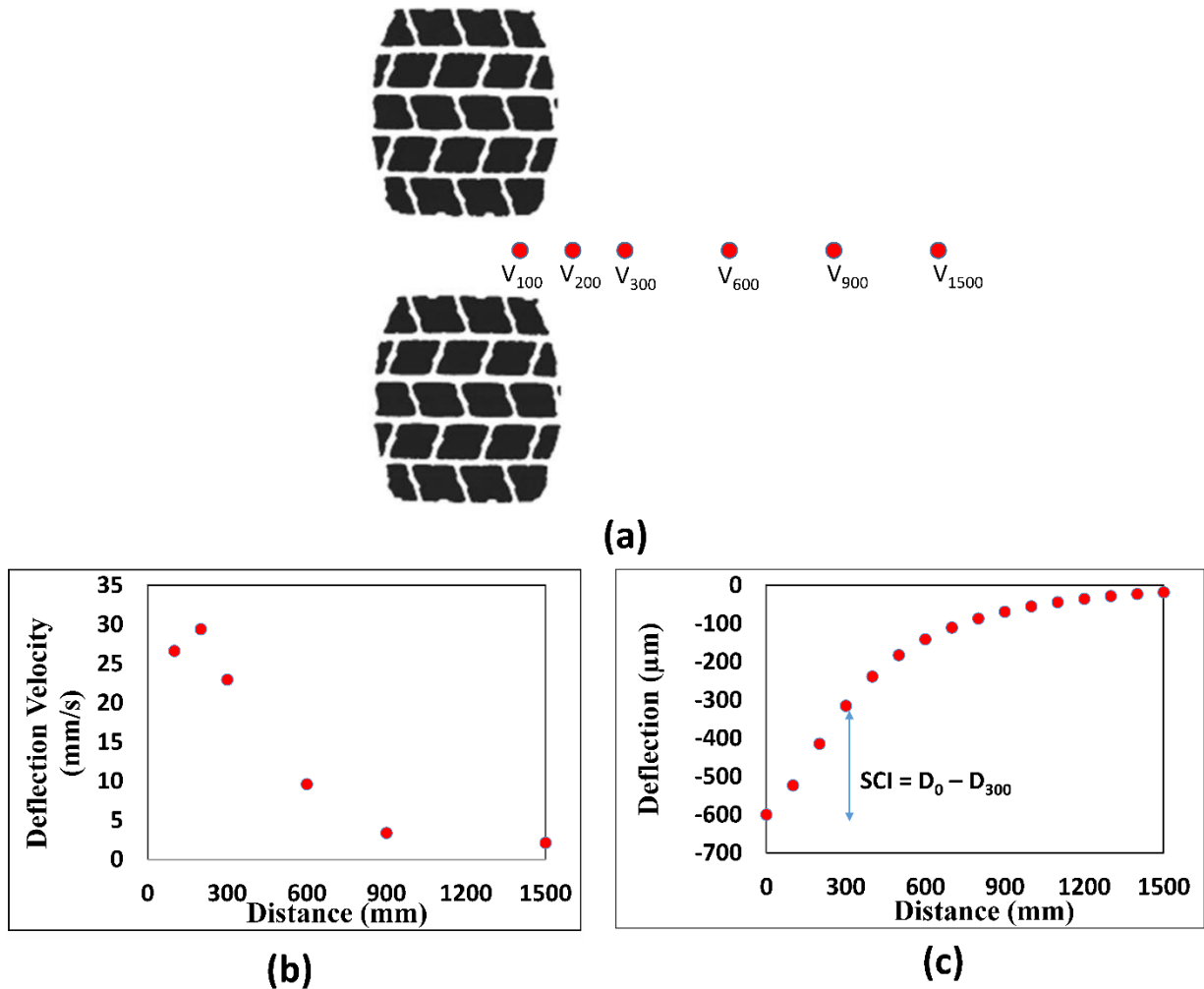


**Figure 1. (a) Doppler laser location between TSD dual tires used in this study (b) measured deflection velocities from TSD sensors (c) computed surface deflections from TSD data**

### The need for temperature adjustment of $SCI_{TSD}$

$SCI_{TSD}$  is known to characterize the strength of the upper portion of a AC pavement structure [11] and, thus, is influenced by asphalt concrete (AC) layer properties such as modulus and thickness. To quantify this statement, a database of 15,000 pavement structures was developed through Monte Carlo simulation. The details regarding the simulation can be found elsewhere [12]. The dataset developed was used to rank the sensitivity of pavement properties (layer modulus and thickness) that affect the  $SCI_{TSD}$  and visualize with a Tornado plot [13]. Figure 2 illustrates the Tornado plot using Spearman's rank-order correlation coefficients between  $SCI_{TSD}$  and pavement properties. The rank-order correlation coefficient measures the strength and direction (negative or positive) of a relationship between two variables.

The rank-order correlation coefficient in Figure 2 is calculated as [13]:

$$r = 1 - \left( \frac{6 \sum (\Delta R)^2}{n(n^2 - 1)} \right) \quad (1)$$

in which,  $\Delta R$  is the difference in the ranks between the input and the output values in the same data

pair and  $n$  is the number of simulations. The effect of the pavement property on the  $SCI_{TSD}$  is high when the absolute value of  $r$  is close to one; when the  $r$  is close to zero, the effect of the variable on  $SCI_{TSD}$  is minimal. The negative correlation for all pavement properties in Figure 2 indicates that an increase in each of the simulated pavement properties reduces the  $SCI_{TSD}$ .

Figure 2 confirms that AC layer thickness ( $r = -0.76$ ) and modulus ( $r = -0.44$ ) are the most sensitive parameters and have higher influence on  $SCI_{TSD}$ . From asphalt rheology, the AC modulus varies with temperature of the asphalt layer; hence, the variation of  $SCI_{TSD}$  with modulus can also be viewed as its sensitivity to temperature. Base thickness ( $r = -0.26$ ) and base modulus ( $r = -0.18$ ) have a moderate impact and subgrade properties have negligible effects on  $SCI_{TSD}$ . In summary, this sensitivity analysis shows that AC layer properties are the most effective parameters to be accounted in temperature adjustment method.

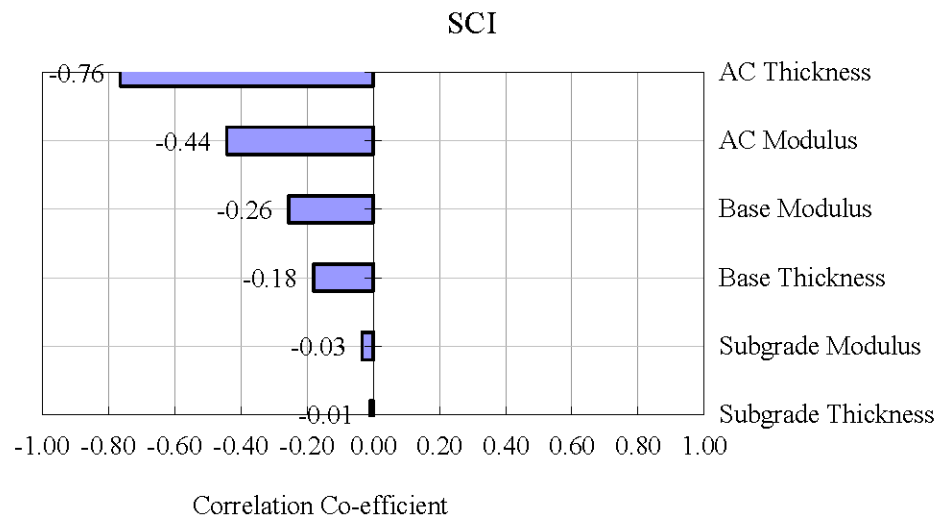


**Figure 2. Sensitivity of pavement properties on  $SCI_{TSD}$**

### Review of available temperature adjustment models

Several models [14- 16] are found in the literature for adjusting SCI measured from FWD to reference temperature. Most of these models are based on empirical relationships with locally calibrated parameters from a limited set of measured SCI and pavement temperatures. However, due to differences in loading configuration (single plate versus dual tires) and mechanism (impact versus moving load) between the FWD and TSD, use of these models with TSD data is questionable.

The authors adopted an interim procedure to address temperature adjustment of  $SCI_{TSD}$  for a recently completed FHWA research study on TSDDs [4]. The model is based on a theoretical model that adjusts asphalt concrete modulus and thus hereafter termed as Stiffness Adjustment Model (SAM).

The model had been modified from its original version and is briefly described in this section.

The steps for this model are:

1. Compute tensile strain at the bottom of the asphalt layer from the measured  $SCI_{TSD}$

$$\varepsilon = a (\text{SCI}_{\text{TSD}})^b \quad (2)$$

where  $a$  and  $b$ , are model parameters shown in Table 1 that depend on the thickness of AC layer. When the thickness is unknown, default values for thin, medium and thick pavements are also provided.

2. Compute the AC layer dynamic modulus at the test temperature,  $E_f$ , based on the calculated strain (Equation 2) using the following equation:

$$E_f = c \times \varepsilon^d \quad (3)$$

where  $c$  and  $d$ , are model parameters shown in Table 1 that depend on the AC layer thickness. When the thickness is unknown, default values for thin, medium and thick pavements are also provided.

3. Compute a temperature adjustment factor,  $T_c$ , for the AC modulus as follows:

$$T_c = \frac{e^{-0.43T_r}}{e^{-0.043T_f}} \quad (4)$$

where  $T_r$  is the reference temperature and  $T_f$  is the AC layer mid-depth temperature at the time of testing.

4. Compute the AC modulus,  $E_r$ , at the selected reference temperature as follows:

$$E_r = \frac{E_f}{T_c} \quad (5)$$

5. Compute the strain,  $\varepsilon_r$ , at the selected reference temperature by rearranging Equation (2) as follows:

$$\varepsilon_r = \left( \frac{E_r}{c} \right)^{\frac{1}{d}} \quad (6)$$

6. Calculate the temperature adjusted  $\text{SCI}_{\text{TSD}}$  using the inverse of Equation 1.

Subsequent field application of the SAM for TSD data collected as part of Transportation Pooled Fund Program TPF-5(282) study [17] identified limitations in the SAM, especially when applied to thin pavement sections. Thus, further examination and refinement of the temperature adjustment model was warranted that led to this study. Firstly, in applying the SAM, the adjustment factors were found to be relatively insensitive to AC layer thicknesses, while as discussed earlier, AC layer thickness has a significant influence on  $\text{SCI}_{\text{TSD}}$  and therefore the adjustment factor is expected to be a function of both AC layer thickness and temperature. Secondly, the LEA approach used in the development of SAM is not able to properly simulate the dynamic pavement response due to moving load, such as TSD loading, and the viscoelastic properties of AC layer. Lastly, SAM methodology can be computationally intensive for network level pavement management application.

To overcome the above limitations, a model based on simulation of TSD dynamic responses with viscoelastic analyses was developed as detailed in the next section.

**Table 1. Model parameters for SAM \***

| AC Layer Thickness                    | SCI <sub>TSD</sub> and maximum tensile strain, equation 2 |          |                       | Strain and AC modulus, equation 3 and 6 |          |
|---------------------------------------|---|----------|-----------------------|---|----------|
|                                       | <i>a</i>  | <i>b</i> | <i>R</i> <sup>2</sup> | <i>c</i>                                | <i>d</i> |
| 76-102 mm<br>(3-4 inches)             | 2.335   | 0.962    | 0.82                  | 3.64E+06                                | -1.27    |
| 102-127 mm<br>(4-5 inches)            | 1.875   | 1.02     | 0.9                   | 4.52E+06                                | -1.36    |
| 127-152 mm<br>(5-6 inches)            | 1.957   | 1.024    | 0.95                  | 4.98E+06                                | -1.44    |
| 152-178 mm<br>(6-7 inches)            | 2.452   | 0.987    | 0.97                  | 4.41E+06                                | -1.46    |
| 178-203 mm<br>(7-8 inches)            | 2.876   | 0.952    | 0.97                  | 3.42E+06                                | -1.46    |
| 203-229 mm<br>(8-9 inches)            | 3.381   | 0.912    | 0.97                  | 3.39E+06                                | -1.51    |
| 229-254 mm<br>(9-10 inches)           | 3.786   | 0.882    | 0.96                  | 2.54E+06                                | -1.49    |
| 254-279 mm<br>(10-11 inches)          | 4.375   | 0.8373   | 0.95                  | 2.27E+06                                | -1.51    |
| 279-305 mm<br>(11-12 inches)          | 4.701   | 0.8103   | 0.94                  | 1.99E+06                                | -1.52    |
| 305-330 mm<br>(12-13 inches)          | 4.905   | 0.7895   | 0.94                  | 1.72E+06                                | -1.53    |
| 330-356 mm<br>(13-14 inches)          | 5.392   | 0.7479   | 0.92                  | 1.59E+06                                | -1.55    |
| 356-381 mm<br>(14-15 inches)          | 5.015   | 0.7594   | 0.94                  | 1.11E+06                                | -1.49    |
| 381- 406 mm<br>(15-16 inches)         | 5.248   | 0.7285   | 0.92                  | 1.00E+06                                | -1.51    |
| Thin<br>76-152 mm<br>(3-6 inches)     | 2.883   | 0.927    | 0.9                   | 9.65E+05                                | -1.072   |
| Medium<br>152- 229 mm<br>(6-9 inches) | 3.071   | 0.935    | 0.97                  | 1.37E+06                                | -1.264   |
| Thick<br>229-406 mm<br>(9-16 inches)  | 4.115   | 0.8412   | 0.94                  | 2.76E+05                                | -1.076   |

\* SCI<sub>TSD</sub> is in  $\mu\text{m}$  and AC modulus is in MPa.

### Viscoelastic analysis model (VEA Model)

A practical model was developed based on viscoelastic (VE) simulation of a range of pavement structures under TSD loading. In the absence of adequate measured TSD data for a range of pavement structures and temperatures to develop an empirical model, viscoelastic simulation of TSD loading provided a more comprehensive and realistic dataset for a device specific temperature adjustment model. 3D-Move program was chosen for the model development since it can account for important factors relevant to this study such as VE characterization of the AC layer and moving

load to generate a dynamic response. Fourier transform technique along with frequency-domain solutions are adopted in 3D-Move to allow the direct use of the frequency sweep test data of AC mixture in the analysis. The program's predicted responses (stresses, strains, and displacements) have been field validated in previous studies [18]. The ability of 3D-Move to simulate the dynamic response of pavement under TSD loading was confirmed in the field trials at the MnROAD test track [4].

A database of 426 pavement structures was generated from the pavement layer properties shown in Table 2. Though, base and subgrade properties have minimal effect on  $SCI_{TSD}$ , the variations of those properties are also considered in the analyses to develop a more complete and representative dataset. A non-uniform tire pressure distribution shown in Figure 3 along with tire grooves was used in the analyses to simulate the TSD loading configuration. The TSD loading was considered as 4080 kg (9 kips) per dual tires. The speed of TSD was set as 48 kph in the analyses, however, the performance of the developed model at different speeds was evaluated in the field validation.

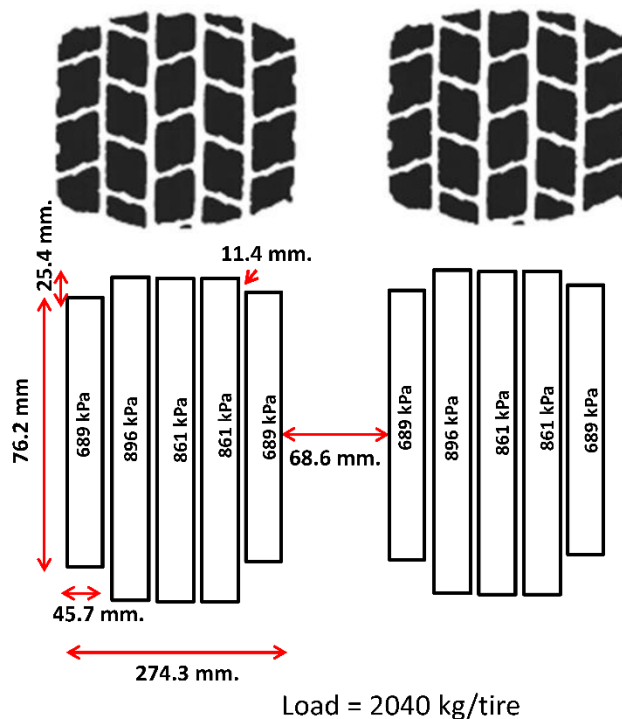


**Figure 3. Non-uniform contact pressure for the TSD in the analyses**

**Table 2. Pavement characterizations used in sensitivity analyses**

| Corresponding Temperature (°C) | Asphalt Thickness (mm) | Base Thickness (mm) | Base Modulus (MPa) | Subgrade Modulus (MPa) |
|--------------------------------|------------------------|---------------------|--------------------|------------------------|
| 0                              | 76                     | 150                 | 138                | 34.5                   |
| 10                             | 127                    | 250                 | 276                | 69                     |
| 20                             | 178                    | 300                 | 552                |                        |
| 30                             | 229                    | 400                 | 1380               |                        |
| 40                             | 279                    | 500                 |                    |                        |
| 50                             | 330                    | 762                 |                    |                        |
|                                | 381                    | 889                 |                    |                        |
|                                |                        | 1016                |                    |                        |

The sensitivity of AC layer dynamic modulus to temperature is a function of AC mix properties, including binder type and mix gradation. To account for variability in the effective parameters, two sets of AC layer properties were used in the study based on freeze and non-freeze climatic regions as defined in Long-Term Pavement Performance (LTPP) study [19]. Data collected as part of LTPP's Specific Pavement Studies (SPS) was utilized to select binder grade and aggregate gradation for freeze and non-freeze climatic regions. Table 3 summarizes the AC layer mix properties used in analyses. The most common binder grade and aggregate gradation in collected LTPP field data were considered as reference properties in analyses. In each climatic region, two additional AC mixes (margin 1 and 2 in Table 3) were also considered in the study to cover the potential range of binder types used in the corresponding regions.

Since the 3D-Move program considers loading rate dependent material properties, dynamic modulus as a function of frequency, commonly known as AC layer master curve, is a key input parameter to the analysis and was generated from the parameters in Table 3 and using AC dynamic modulus equation [20].

$$\log E^* = -1.25 + 0.029\rho_{200} - 0.0018(\rho_{200})^2 - 0.0028\rho_4 - 0.058V_a - 0.822 \frac{V_{beff}}{V_{beff}+V_a} + \frac{3.872-0.0021\rho_4+0.003958(\rho_{38})-0.000017(\rho_{38})^2+0.0055\rho_{34}}{1+e^{(-0.603313-0.313351\log(f)-0.393532\log(\eta))}} \quad (7)$$

where  $E^*$  = dynamic modulus of mix,  $10^5$  psi

$\eta$  = viscosity of binder,  $10^6$  poise

$f$  = loading frequency, Hz

$\rho_{200}$  = % passing #200 (0.075 mm) sieve

$\rho_4$  = cumulative % retained on #4 (4.76 mm) sieve

$\rho_{38}$  = cumulative % retained on 3/8 in. (9.5 mm) sieve

$\rho_{34}$  = cumulative % retained on 3/4 in. (19 mm) sieve

$V_a$  = air void, % by volume

$V_{beff}$  = effective binder content, % by volume

The viscosity can be calculated as a function of temperature based on  $A$  and  $VTS$  viscosity temperature susceptibility [21] as follows:

$$\log \log \eta = A + VTS \cdot \log T_R \quad (8)$$

where  $\eta$  = the viscosity, cP

$T_R$  = the temperature at which the viscosity is estimated, Rankine

$A$  = Regression Intercept

$VTS$  = Regression slope of viscosity temperature susceptibility

**Table 3. Binder grade and material gradation used in sensitivity analyses**

| AC Mix Properties                  | Freeze Margin 1 | Freeze Reference | Freeze Margin 2 | Non - Freeze Margin 1 | Non - Freeze Reference | Non - Freeze Margin 2 |
|------------------------------------|-----------------|------------------|-----------------|-----------------------|------------------------|-----------------------|
| Performance Grade (PG)             | 58-34           | 64-22            | 70-16           | 58-28                 | 70-22                  | 76-16                 |
| Binder — Regression Intercept      | 10.035          | 10.98            | 10.641          | 11.01                 | 10.299                 | 10.015                |
| Binder—VTS                         | -3.35           | -3.68            | -3.548          | -3.701                | -3.426                 | -3.315                |
| Air Voids (Percent)                | 4               | 4                | 4               | 5.5                   | 5.5                    | 5.5                   |
| Effective Binder Content (Percent) | 6               | 6                | 6               | 5                     | 5                      | 5                     |
| Percent Passing #200 Sieve         | 4               | 4                | 4               | 4                     | 4                      | 4                     |
| Percent Retained #4 Sieve          | 49              | 49               | 49              | 50                    | 50                     | 50                    |
| Percent Retained 9.5 mm Sieve      | 28              | 28               | 28              | 23                    | 23                     | 23                    |
| Percent Retained 19 mm Sieve       | 6               | 6                | 6               | 4                     | 4                      | 4                     |

Figure 4 depicts the master curve at different AC layer temperatures corresponding to reference AC mix properties of ‘freeze’ climatic region detailed in Table 3. The figure illustrates that the temperature has a significant effect on AC modulus. Similar master curves were developed for each AC mix in Table 3.

The input variables shown in Table 2 are sampled based on AC and base layer thickness of typical pavement sections to minimize the number of VE analyses. In all, a dataset of 426 pavement sections with corresponding  $SCI_{TSD}$  was developed using VE analyses with TSD loading configuration.

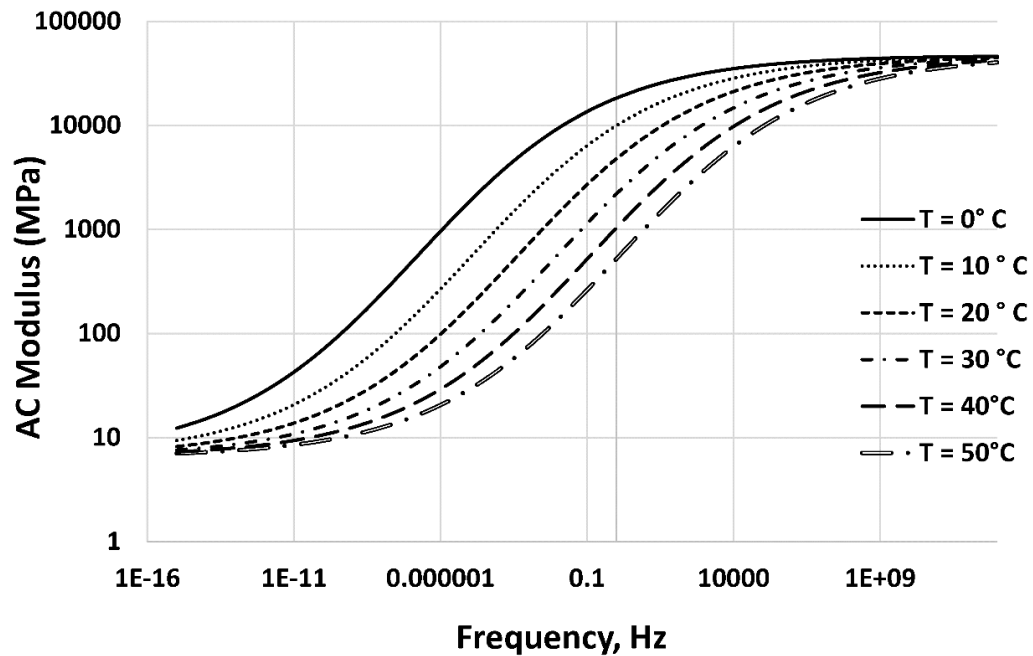


**Figure 4. Dynamic modulus at different temperatures for reference AC mix of ‘freeze’ region used in analyses.**

From Figure 2, the temperature adjustment model should include parameters reflecting AC layer thickness and modulus. The temperature sensitivity of the AC modulus arises from the binder type used in the AC mix. Lukanen et al. [16] used latitude as a surrogate for binder modulus or grade in a temperature adjustment model for SCI from FWD. Similarly, to account for binder grade in the proposed VEA model, the PG binder used in analyses were transformed to latitude using LTPPBind online program [22] that select PG binder based on the altitude of the location. The program recommends PG binder for the specific site based on site temperature condition after adjustment for traffic loading and speed. Table 4 shows latitude from LTPPBind corresponding to the PG binder used in dataset.

**Table 4. Latitudes for binder PG used in analyses**

|          |       |       |       |       |       |       |
|----------|-------|-------|-------|-------|-------|-------|
| PG-grade | 58-34 | 64-22 | 70-16 | 58-28 | 70-22 | 76-16 |
| Latitude | 47.96 | 47.73 | 40.93 | 40.63 | 43.10 | 38.56 |

SCI<sub>TSD</sub> computed from the VE analyses were utilized to develop VEA model in following steps:

1. Adjustment factors defined as the ratio of SCIs at a reference temperature (e.g. 25 °C) to the SCIs at other temperatures ( $SCI_{Ref}/SCI_T$ ) were estimated.
2. An adjustment factor model with functional form inspired by Lukanen et al. [16] was defined with the most effective parameters on SCI (AC layer thickness, temperature and latitude of test location). The model was then calibrated with calculated adjustment factors from the VE analyses (step 1).

Equation (9) shows the temperature adjustment factor model for SCI<sub>TSD</sub>. It should be noted that

proposed equation can be used with any reference temperature.

$$\lambda = \frac{SCI_{Ref}}{SCI_T} = \frac{10^{-0.05014T_{Ref}+0.019049T_{Ref}\log(h_{AC})\log(\varphi)}}{10^{-0.05014T+0.019049T\log(h_{AC})\log(\varphi)}} \quad (9)$$

where  $\lambda$  = Temperature adjustment factor

$SCI_{Ref}$  = Adjusted  $SCI_{TSD}$  at reference temperature

$T_{Ref}$  = Reference temperature, °C

$T$  = Mid-depth AC layer temperature at time of measurement, °C

$h_{AC}$  = Asphalt layer thickness, mm

$\Phi$  = Latitude of location of measurement (within 30 to 50 degrees)

Since the latitudes (as substitute of binder grades) in the database were chosen based on LTPPBind recommendation, Equation (9) is only applicable for test locations within the US. However, the model can also be extended to test sites outside the US. To assess global application, step 2 was repeated excluding latitude of test location and the equation was recalibrated as shown in Equation (10).

$$\lambda = \frac{SCI_{Ref}}{SCI_T} = \frac{10^{-0.0521T_{Ref}+0.0322T_{Ref}\log(h_{AC})}}{10^{-0.0521T+0.0322T\log(h_{AC})}} \quad (10)$$

The base and subgrade properties are not included in the equations since they have minimal effect on  $SCI_{TSD}$  (Figure 2) and also that these properties are generally unavailable at network level pavement management systems (PMS). However, as described earlier, the dataset used for model development accounts for variations of base and subgrade properties to ensure that the model is applicable to range of pavement structures.

Figure 5 shows the temperature adjustment factors for various asphalt layer thicknesses from the VEA and SAM models. Similar trends were observed for all AC mixes in Table 3. However, for brevity, only ‘non-freeze’ region’s reference AC mix is shown in the figure. Adjustment factors from SAM are similar in different AC layer thickness whereas VEA adjustment factors are sensitive to both temperature (AC layer modulus) and AC layer thickness. Field validation of the VEA model with TSD data is detailed in the next section.

### Field evaluation of VEA model

Data from the TSD trials at the MnROAD pavement test track facility [4] and one pavement section each in Virginia and Illinois [17] were used to validate the US equation (Equation (9)). Repeat TSD testing were conducted over the same pavement sections during morning and afternoon within a day or two providing deflection data at two different AC layer temperatures. The TSD deflections are averaged and reported over 10-m interval and the  $SCI_{TSD}$  at the two different temperatures are shown in Figure 6. The surface temperatures were measured during data collection and the BELLS equation was used to estimate the mid-depth pavement layer temperatures [16].

Figure 6A shows measured  $SCI_{TSD}$  at the MnROAD mainline section that consists of multiple pavement cells subjected to live traffic as part of Interstate 94 near Albertville, MN. The data shown in this figure comprises flexible pavement cells with AC layer thicknesses of 76 and 127 mm. The TSD trial shown in the figure represents the data collected at a speed of 90 kph and dual tire load of 5048 kg (11 kips). The average mid-depth pavement layer temperatures were 25°C

and 32°C in the morning and afternoon, respectively. Figure 6B shows measured  $SCI_{TSD}$  at two temperatures (32°C and 39°C) of a flexible pavement section with AC layer thickness of 190 mm that is part of US-29 near Altavista, VA. In this location, the average speed of TSD was 82 kph with dual tire load of 4082 kg (9000 kips). Finally, measured  $SCI_{TSD}$  of a pavement section with AC layer thickness of 286 mm collected at a section of road in Interstate 57 near Champaign, IL at two AC layer temperatures of 22°C and 30°C are shown in Figure 6C. The average TSD speed was 93 kph and TSD dual tire load was recorded as 4445 kg (9800 lb).

The VEA model (Equation (9)) was used to adjust measured  $SCI_{TSD}$  at these locations. Figure 7 shows adjusted  $SCI_{TSD}$  from the VEA model. The adjusted  $SCI_{TSD}$  from morning and afternoon measurements show good agreement. The agreement between adjusted  $SCI_{TSD}$  from VEA model were evaluated using paired-t-test for differences in means. This test was selected since it considers model error and eliminates the random differences due to equipment error. Test statistic for each site was calculated using the following equation considering zero differences between adjusted  $SCI_{TSD}$ 's as the null hypothesis:

$$test\ statistic = \frac{\overline{X}_D}{\frac{S_D}{\sqrt{n}}} \quad (11)$$

where  $\overline{X}_D$  is average of differences between adjusted  $SCI_{TSD}$ ,  $S_D$  is standard deviation of those differences and  $n$  is number of measurements.

The values of  $t$  critical are selected at 99.9% confidence of interval and number of paired measurements. Test statistic and  $t$  critical for all locations are shown in Figure 7 and in all cases, the test statistic is less than the critical value indicating non-rejection of the null hypothesis. Consequently, it can be concluded that the VEA model successfully adjusted the  $SCI_{TSD}$  measurements at different temperatures in different pavement structures and vehicle speed. In addition, the data from MnROAD mainline was used to verify the accuracy of the VEA model. In this pavement section, the  $SCI_{TSD}$  measured in the morning can be considered as reference since the measurement was taken close to 25°C. The close agreement between adjusted  $SCI_{TSD}$  measured in the afternoon with the measured  $SCI_{TSD}$  in the morning in Figure 7a verifies the accuracy of VEA model.

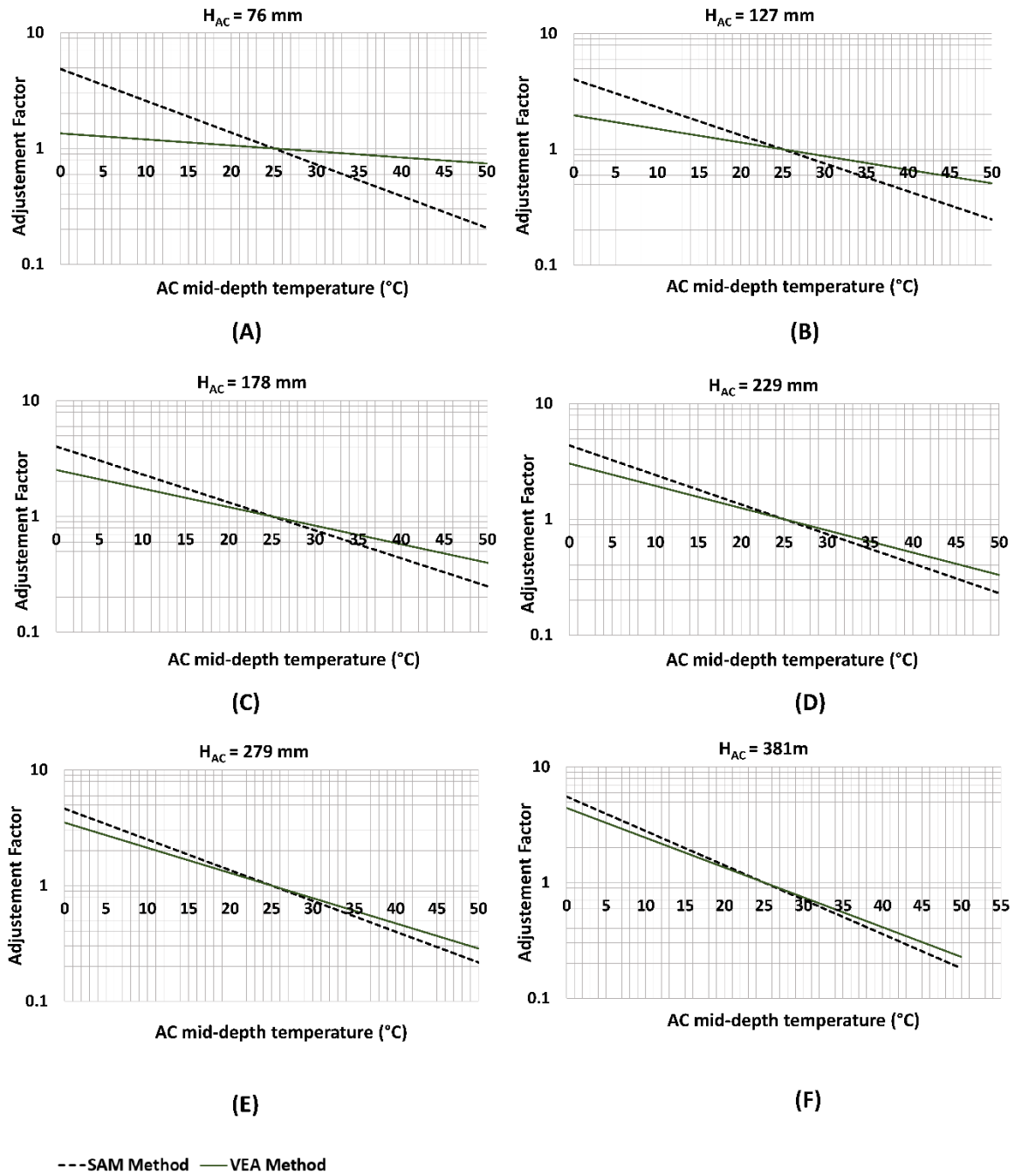


**Figure 5. Comparison of adjustment factors computed from SAM and VEA models in various asphalt layer thickness using non-freeze reference material properties.**

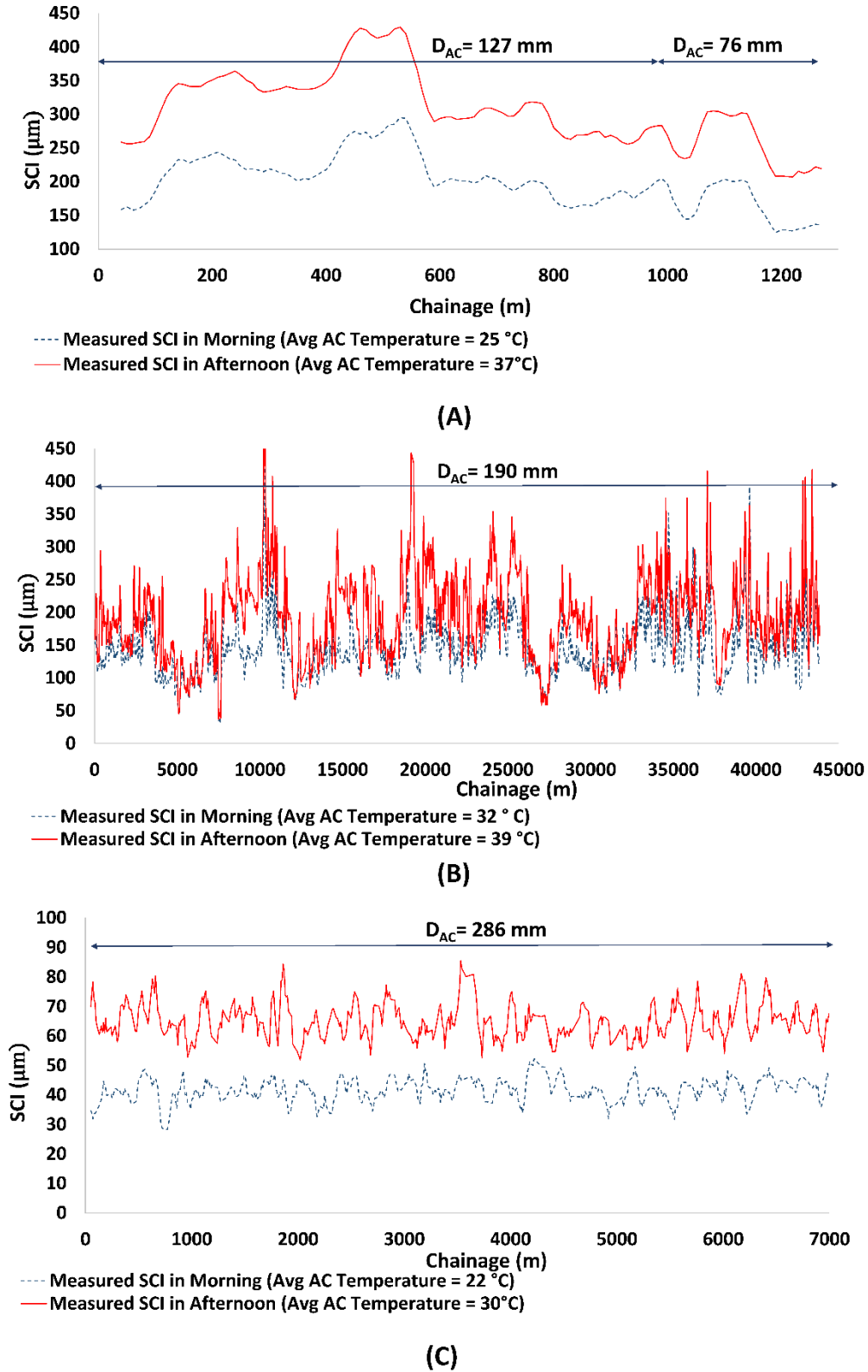
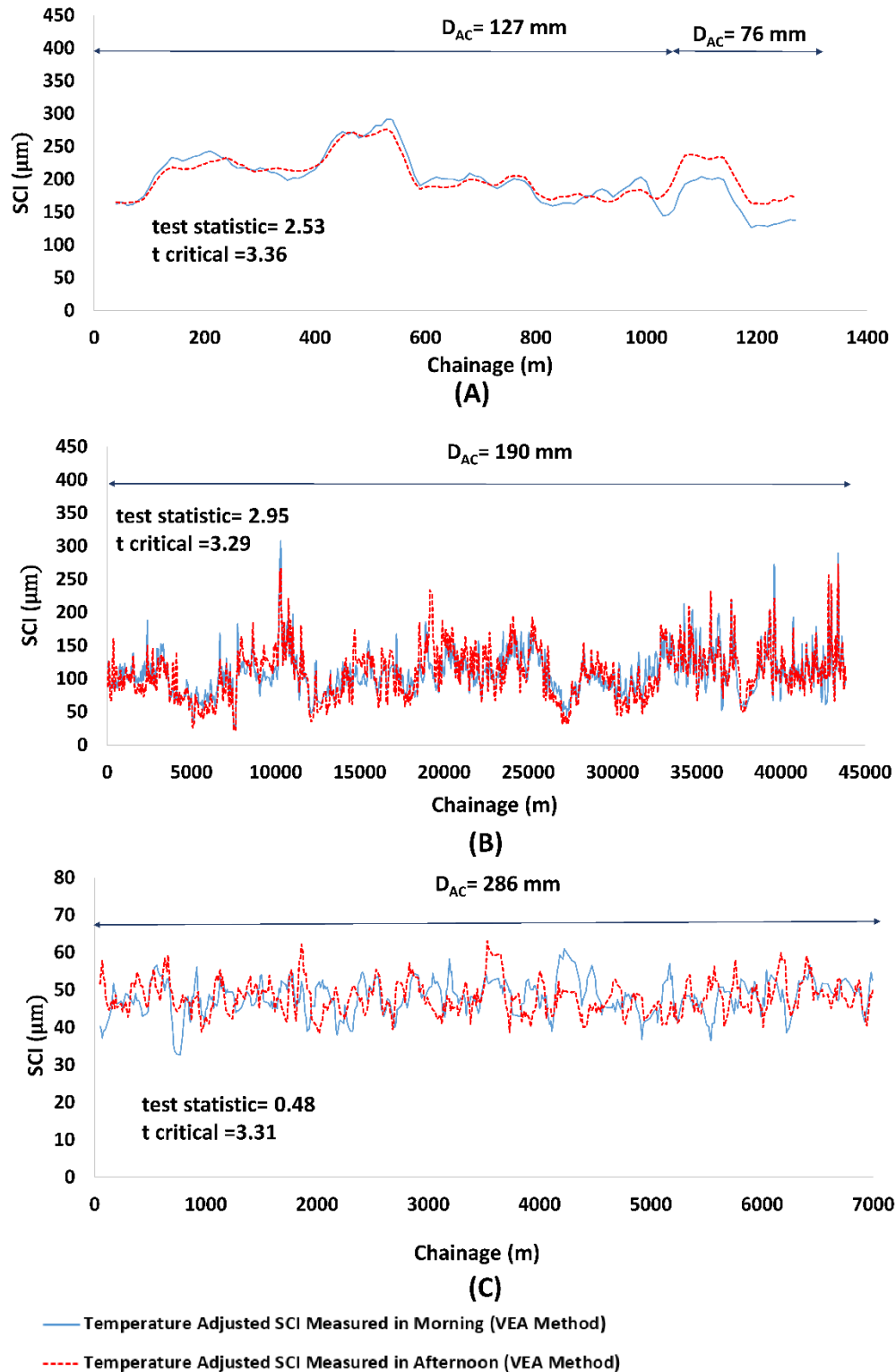
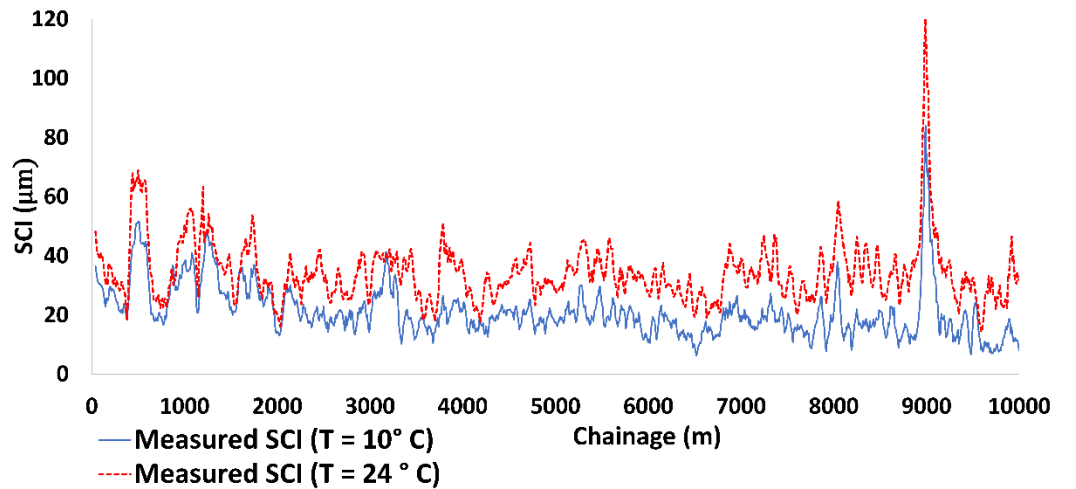


Figure 6. Measured SCI<sub>TSD</sub> at two temperatures at (A) MnROAD facility Interstate 94 near Albertville, MN (B) US-29 near Altavista, VA and (C) Interstate 57 near Champaign, IL

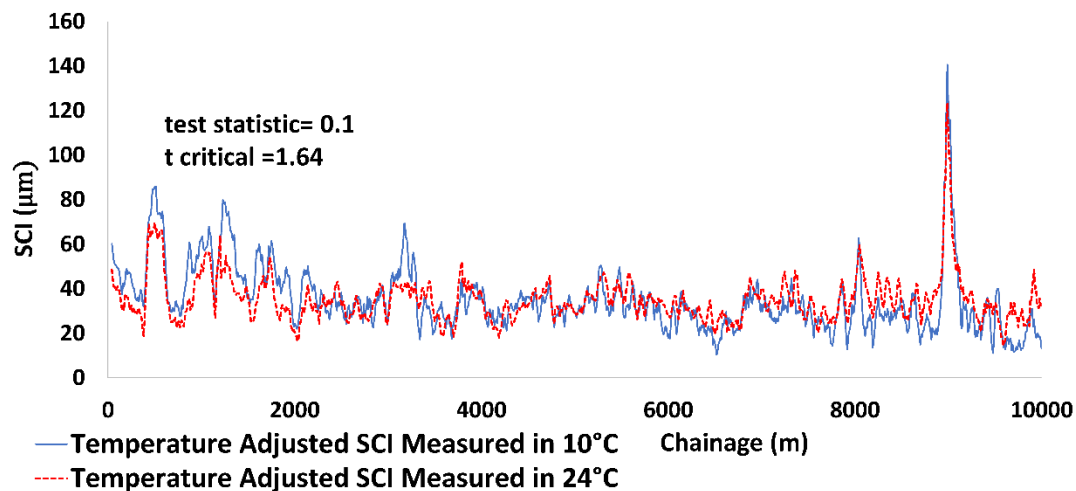


**Figure 7. Adjusted SCI<sub>TSD</sub> for temperature from TSD using VEA model at (A) MnROAD facility Interstate 94 near Albertville, MN (B) US-29 near Altavista, VA and (C) Interstate 57 near Champaign, IL**

TSD data collected in sections pavements in Europe and Australia were used to evaluate the proposed equation for temperature adjustment factor for  $SCI_{TSD}$  outside of US (Equation (10)). As shown in Figure 8, the model effectively adjusted  $SCI_{TSD}$  to a reference temperature for the dataset collected at a pavement section at Europe.



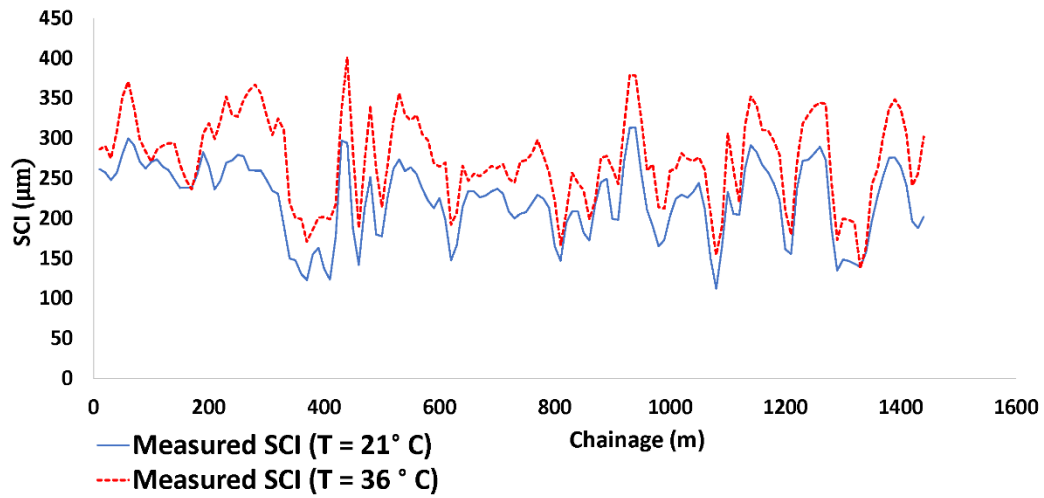
(A)



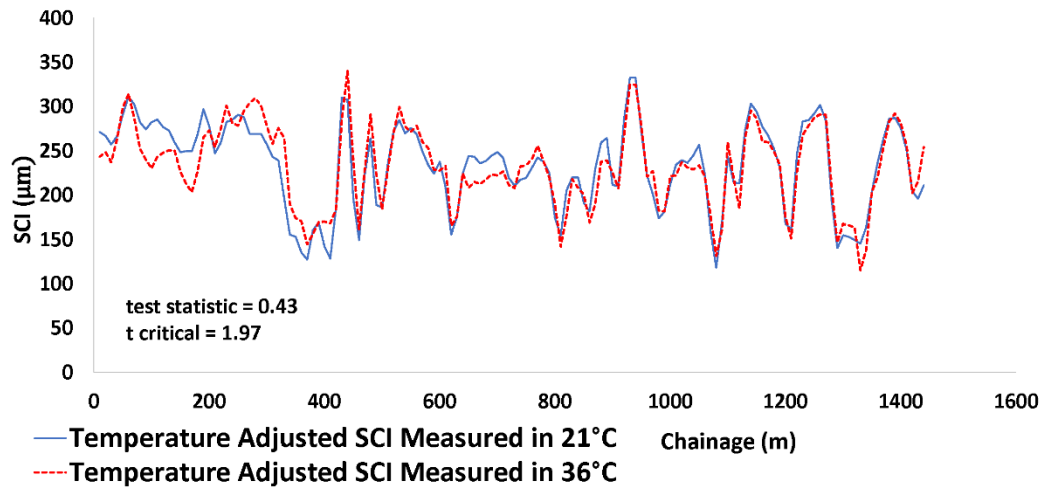
(B)

**Figure 8. (A) Measured  $SCI_{TSD}$  in two temperatures in a pavement section at Europe (B) adjusted  $SCI_{TSD}$  using VEA model**

The VEA model was also used to adjust SCIs from TSD data collected along Deception Bay Road, Queensland, in Australia. Figure 9 shows measured and temperature adjusted SCIs at this location. As shown in the figure, the model provides reasonable performance to adjust measured SCIs to a reference temperature.



(A)



(B)

**Figure 9. (A) Measured  $SCI_{TSD}$  in two temperatures along Deception Bay Road in Australia (B) adjusted  $SCI_{TSD}$  using VEA model**

## Conclusion

Traffic speed deflection devices, such as TSD, are increasingly becoming effective and practical tools for structural evaluation of in-service pavements, especially for network level pavement management applications.  $SCI_{TSD}$  is globally used as an indicator of structural condition of bound layers of flexible pavement structures and to estimate remaining structural capacity. Knowledge of remaining and required structural life would help pavement engineers in determining the right time for rehabilitation treatments. Since asphalt materials are sensitive to temperature, measured  $SCI_{TSD}$  is highly affected by pavement temperature at the time of data collection. A pertinent temperature adjustment model would enable the use of  $SCI_{TSD}$  to track pavement structural performance over time and across sections.

A parametric sensitivity analysis revealed that asphalt layer properties (thickness and temperatures) are the most sensitive parameters affecting  $SCI_{TSD}$ . VE analyses were performed on a range of asphalt layer temperatures and pavement layer properties to develop a robust dataset of dynamic pavement responses under TSD moving load. The dataset was then used to develop a temperature adjustment model for  $SCI_{TSD}$  called VEA model. The VEA model accounts for all sensitive parameters including asphalt layer thickness, temperatures (or modulus) and binder type. The VEA model was successfully field validated with TSD data collected in three locations within the US - MnROAD pavement test track facility and one in-service pavement section each in Virginia and Illinois – and two locations outside the US, one location each in Europe and Australia.

## Acknowledgement

This research was performed while the first author held National Research Council (NRC) Research Associateship award at Federal Highway Administration and their support is greatly acknowledged. The authors would also like to thank Dr. Adam Zofka of Road and Bridge Research Institute (IBDiM), Poland, and Mr. Richard Wix of ARRB Group, Australia, for sharing TSD data collected in Europe and Australia, respectively.

## References

1. Xu, B., Ranji Ranjithan, S., & Richard Kim, Y. New relationships between falling weight deflectometer deflections and asphalt pavement layer condition indicators. *Transportation Research Record: Journal of the Transportation Research Board*, No. 1806(1), 2002, pp.48-56.
2. Hossain, A. S. M. M., and J. P. Zaniewski. Characterization of falling weight deflectometer deflection basin. *Transportation Research Record: Journal of the Transportation Research Board*, No. 1293, 1991, pp. 1–11.
3. DRAFT TRH12. Technical Recommendation for Highways: *Flexible pavement rehabilitation investigation and design*. Department of Transport Private Bag X193 PRETORIA 0001 Republic of South Africa, 1997.
4. Rada, G. R., Nazarian, S., Visintine, B. A., Siddharthan, R. and Thyagarajan, S. *Pavement structural evaluation at the network level*. Federal Highway Administration Report FHWA-HRT-15-074, Washington. D.C., 2016.
5. Nasimifar, M., Thyagarajan, S., and Sivaneswaran, S.” Computation of pavement vertical surface deflections from Traffic Speed Deflectometer data – evaluation of current methods.” *Journal of Transportation Engineering, Part B: Pavements, ASCE*, 2017a.

6. Zofka, A., Sudyka, J., Maliszewski, M., Harasim, P., & Sybilski, D. Alternative approach for interpreting traffic speed deflectometer results. *Transportation Research Record: Journal of the Transportation Research Board*, (2457), 2017, pp.12-18.
7. Katicha, S., Flintsch, G., Shrestha, S., and Thyagarajan, S. *Demonstration of network level pavement structural evaluation with traffic speed deflectometer: Final Report*, Transportation Pooled Fund Program TPF 5(282), 2017.  
<http://www.pooledfund.org/Details/Study/518>
8. Soren, R., Lisbeth, A., Susanne, B., & Jorgen, K. *A comparison of two years of network level measurements with the Traffic Speed Deflectometer*, Transport Research Arena Europe 2008, Ljubljana, Slovenia, 2008.
9. Březina, I., Stryk, J., & Grošek, J. Using traffic speed deflectometer to measure deflections and evaluate bearing capacity of asphalt road pavements at network level. *In IOP Conference Series: Materials Science and Engineering* (Vol. 236, No. 1, p. 012102). IOP Publishing, 2017.
10. Baltzer, S. Three years of high speed deflectograph measurements of the danish state road network. *In Bearing Capacity of Roads, Railways and Airfields. 8th International Conference* (BCR2A'09), 2009.
11. Horak E. The use of surface deflection basin measurements in the mechanistic analysis of flexible pavements. *Proc., Vol. 1, Sixth International Conference Structural Design of Asphalt Pavements*, University of Michigan, Ann Arbor, Michigan, USA, 1987.
12. Nasimifar, M., Thyagarajan, S., Siddharthan, R. V., and Sivaneswaran, S. Robust deflection indices from traffic speed deflectometer measurements to predict critical pavement responses for network level PMS application. *Journal of Transportation Engineering, ASCE*, 04016004, 2016.
13. Vose, D. *Quantitative risk analysis: a guide to Monte Carlo simulation modelling*. John Wiley & Sons. New York, USA, 1997.
14. Kim, Y. R., B. O. Hibbs, and Y. C. Lee. Temperature correction of deflections and backcalculated asphalt concrete moduli. *Transportation Research Record: Journal of the Transportation Research Board*, No.1473, 1995, pp. 55–62
15. Kim, Y. Richard, and Park, Heemun. *Use of falling weight deflectometer multi-load data for pavement strength estimation*. (Report No. FHWA/NC/2002-006 for the North Carolina Department of Transportation). Raleigh NC, 2002.
16. Lukanen, E. O., Stubstad, R., & Briggs, R. *Temperature predictions and adjustment factors for asphalt pavement*. Federal Highway Administration Report, FHWA-RD-98-085, Washington, DC., 2000.
17. Transportation Pooled Fund Program. <http://www.pooledfund.org/Details/Study/518>, Accessed April. 30, 2018.
18. Siddharthan, R.V., El-Mously, M., Krishnamenon, N., and Sebaaly, P.E. Validation of a pavement response model using full-scale field tests. *International Journal of Pavement Engineering*, Vol. 3(2), 2002, pp. 85-93.
19. Long-Term Pavement Performance (LTPP) InfoPave: <https://infopave.fhwa.dot.gov>. Accessed April. 30, 2018.
20. Witczak, M. W., & Bari, J. *Development of a master curve (E\*) database for lime modified asphaltic mixtures*, Arizona State University Research Report, Tempe (Arizona, USA): Arizona State University, 2004.
21. Velasquez, R., Hoegh, K., Yut, I., Funk, N., Cochran, G., Marasteanu, M., and

- Khazanovich, L. *Implementation of the MEPDG for new and rehabilitated pavement structures for design of concrete and asphalt pavements in minnesota*. Report No. MN/RC 2009-06, Minnesota Department of Transportation, St. Paul, MN, 2009.
22. LTPPBind Online Program. <https://infopave.fhwa.dot.gov/Tools/LTPPBindOnline>, Accessed April. 30, 2018.